Drone-based vertical profiling of particulate matter size distribution and carbonaceous aerosols: urban vs. rural environment

Kajal Julaha[1,2,*], Vladimír Ždímal[2], Saliou Mbengue[3], David Brus[4], Naděžda Zíková[2,5,*]

[1]Department of Atmospheric Physics, Faculty of Mathematics and Physics, Charles University, Prague, 18000, Czech Republic.

[2]Institute of Chemical Process Fundamentals of the Czech Academy of Sciences, Prague 16500, Czech Republic.

[3]Global Change Research Institute of the Czech Academy of Sciences, Brno 60300, Czech Republic.

[4]Atmospheric Composition Research, Finnish Meteorological Institute, Helsinki 00560, Finland.

[5]Institute for Environmental Studies, Faculty of Sciences, Charles University, Prague, 12801, Czech Republic

*Correspondence to: zikova@icpf.cas.cz (Naděžda Zíková), julaha@icpf.cas.cz (Kajal Julaha)

Keywords: Equivalent black carbon, vertical distributions, Drone, micro-aethalometer AE51, optical particle counter, Aethalometer AE33, optical particle sizer, humidity control.
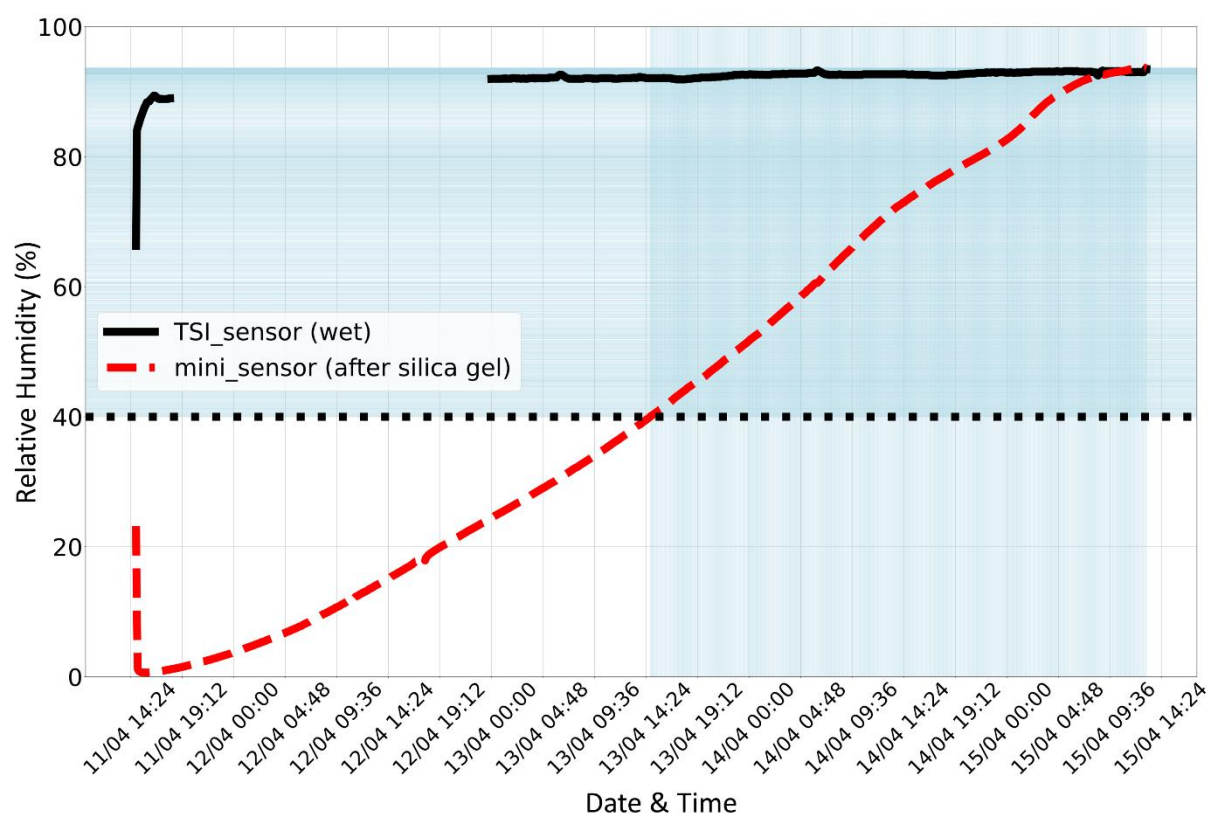
Figure S1. Variation of Relative Humidity after subjecting Air stream Dryer to 100 % RH.
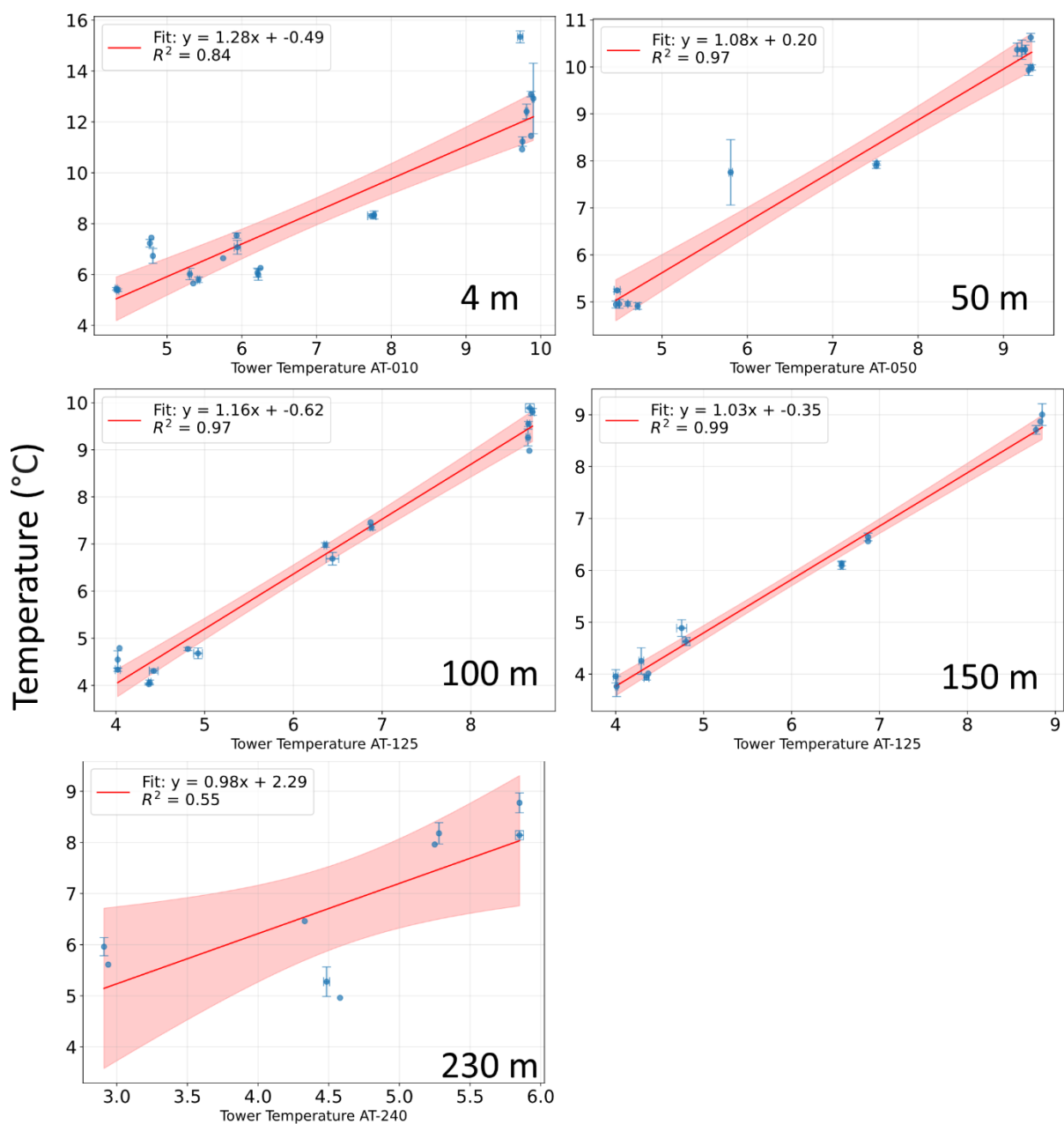
Figure S2. Correlation plot between temperature measurements obtained from the sensor SHT85 placed on the drone with OPC and from the sensors on the tower at various heights.
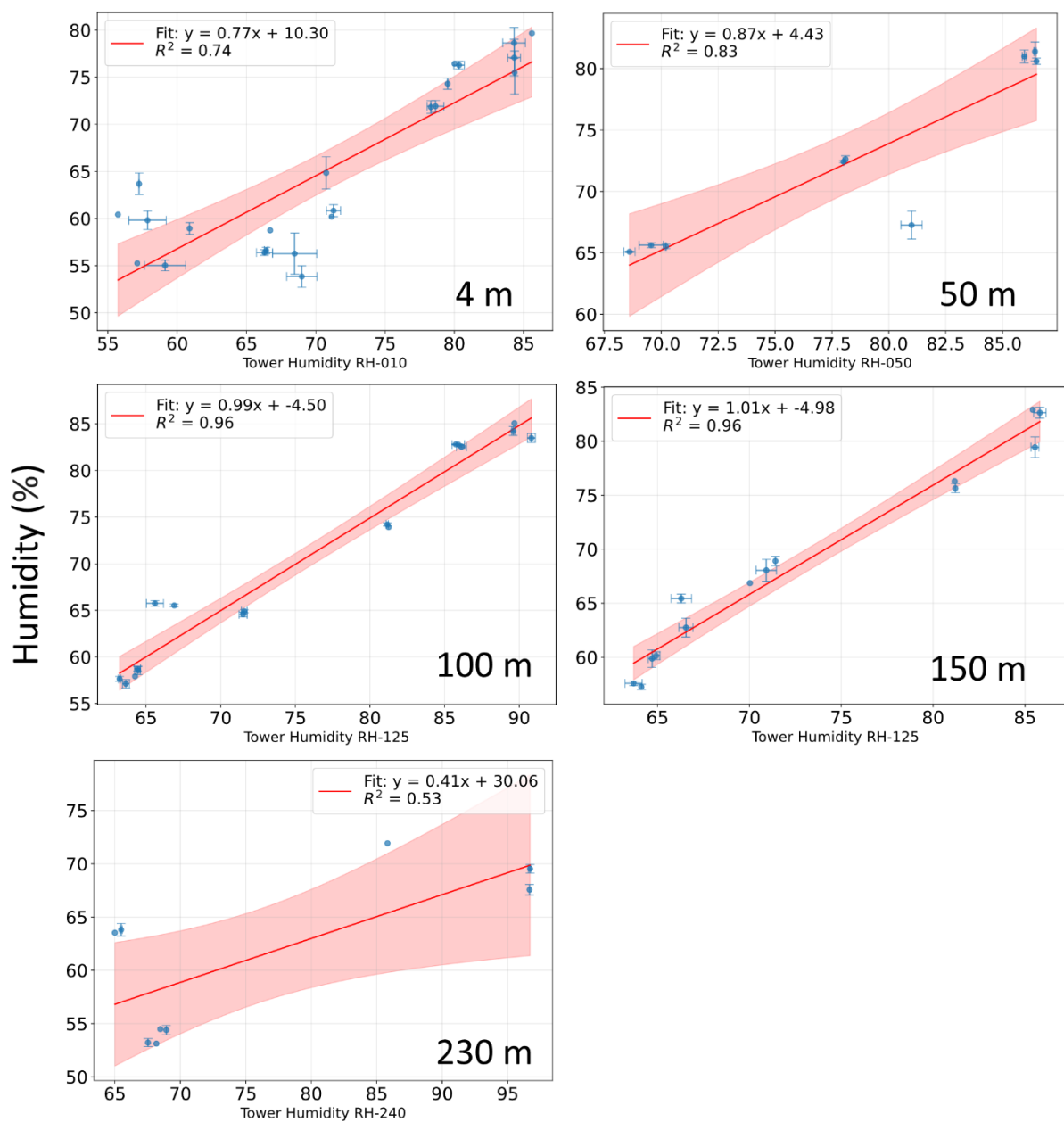
Figure S3. Correlation plot between relative humidity measurements obtained from the sensor SHT85 placed on the drone with OPC and from the sensors on the tower at various heights.

28
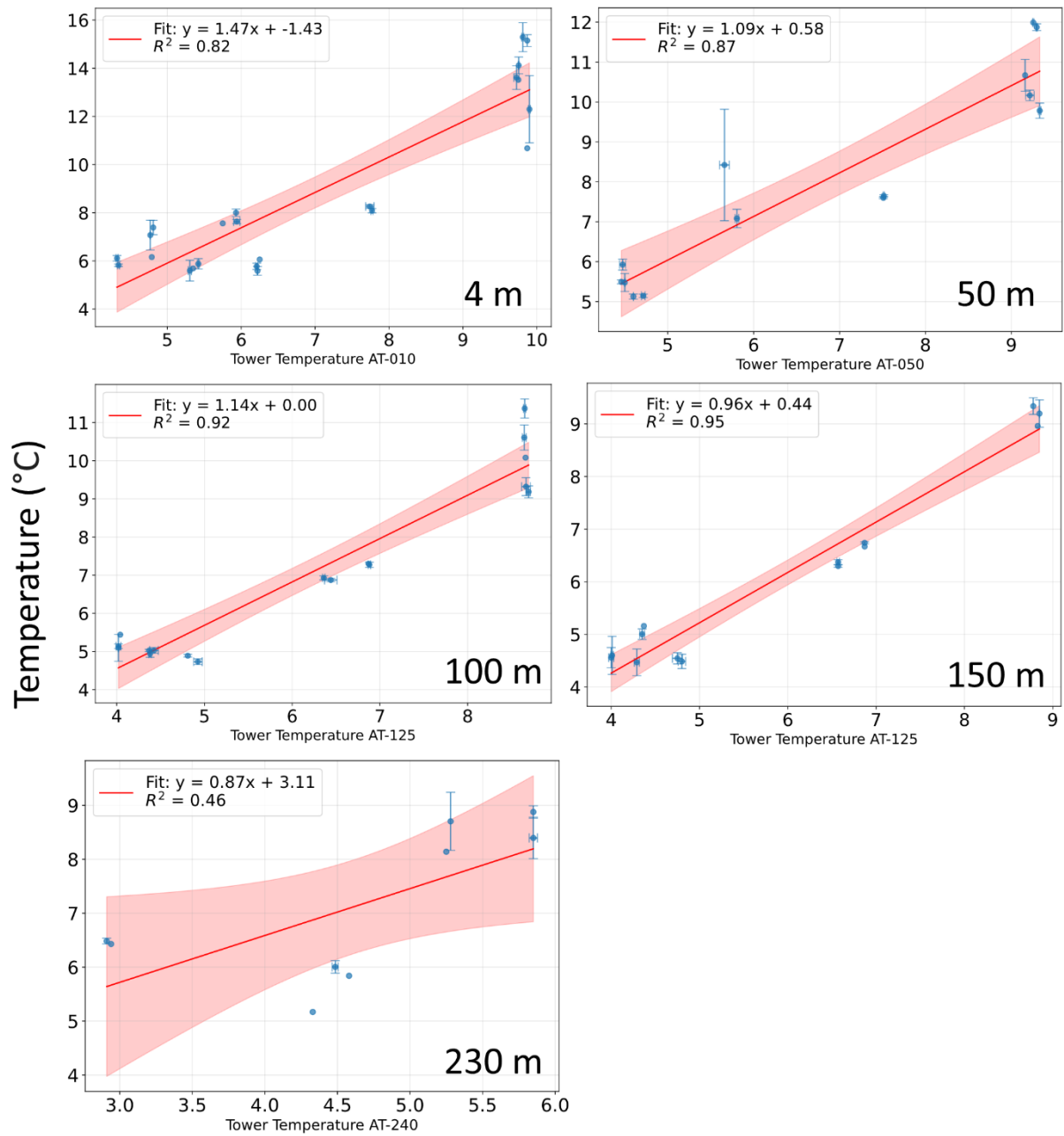
Figure S4. Correlation plot between temperature measurements obtained from the sensor BME placed on the drone with OPC and from the sensors on the tower at various heights.

31
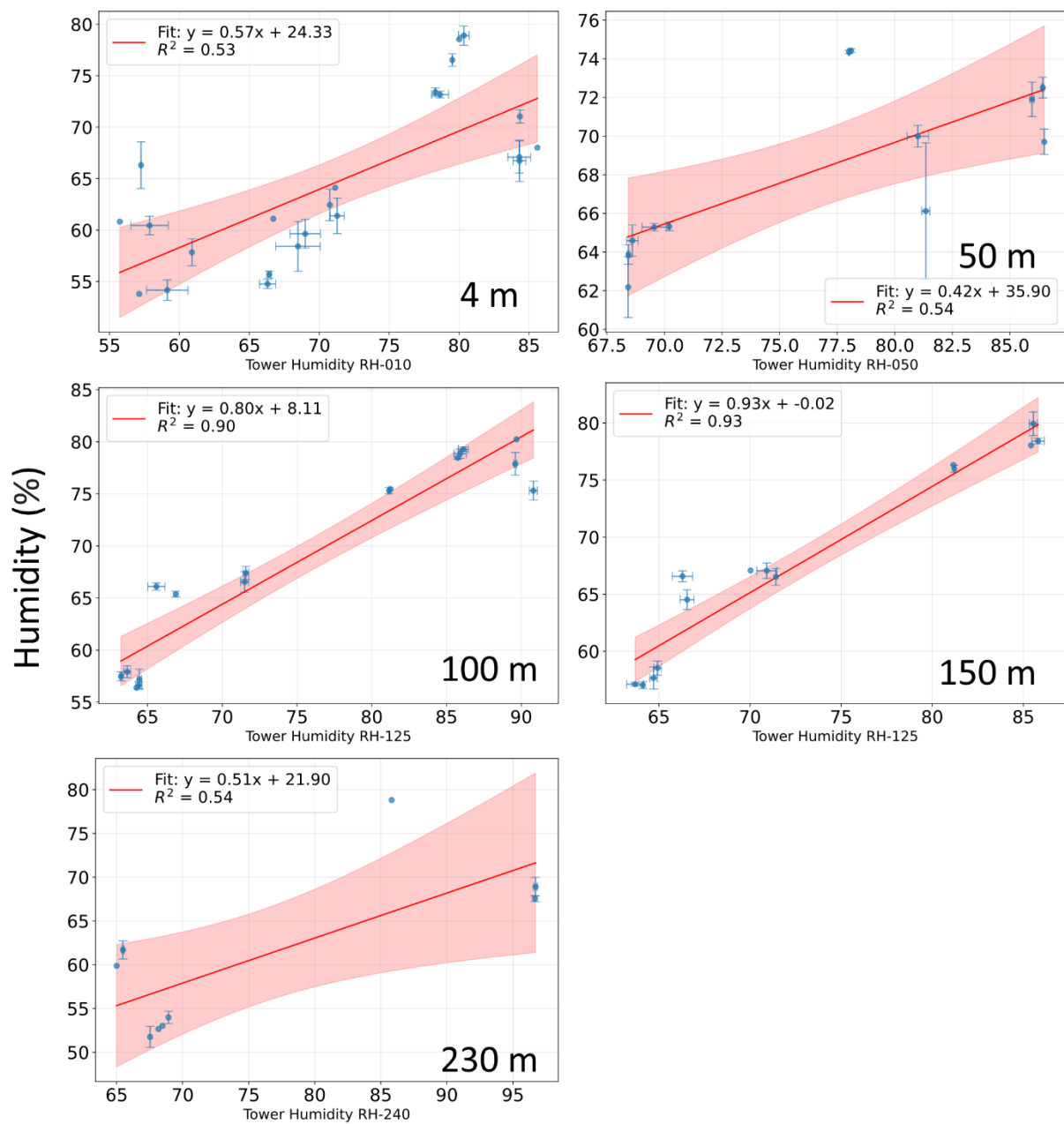
Figure S5. Correlation plot between relative humidity measurements obtained from the sensor BME placed on the drone with OPC and from the sensors on the tower at various heights.
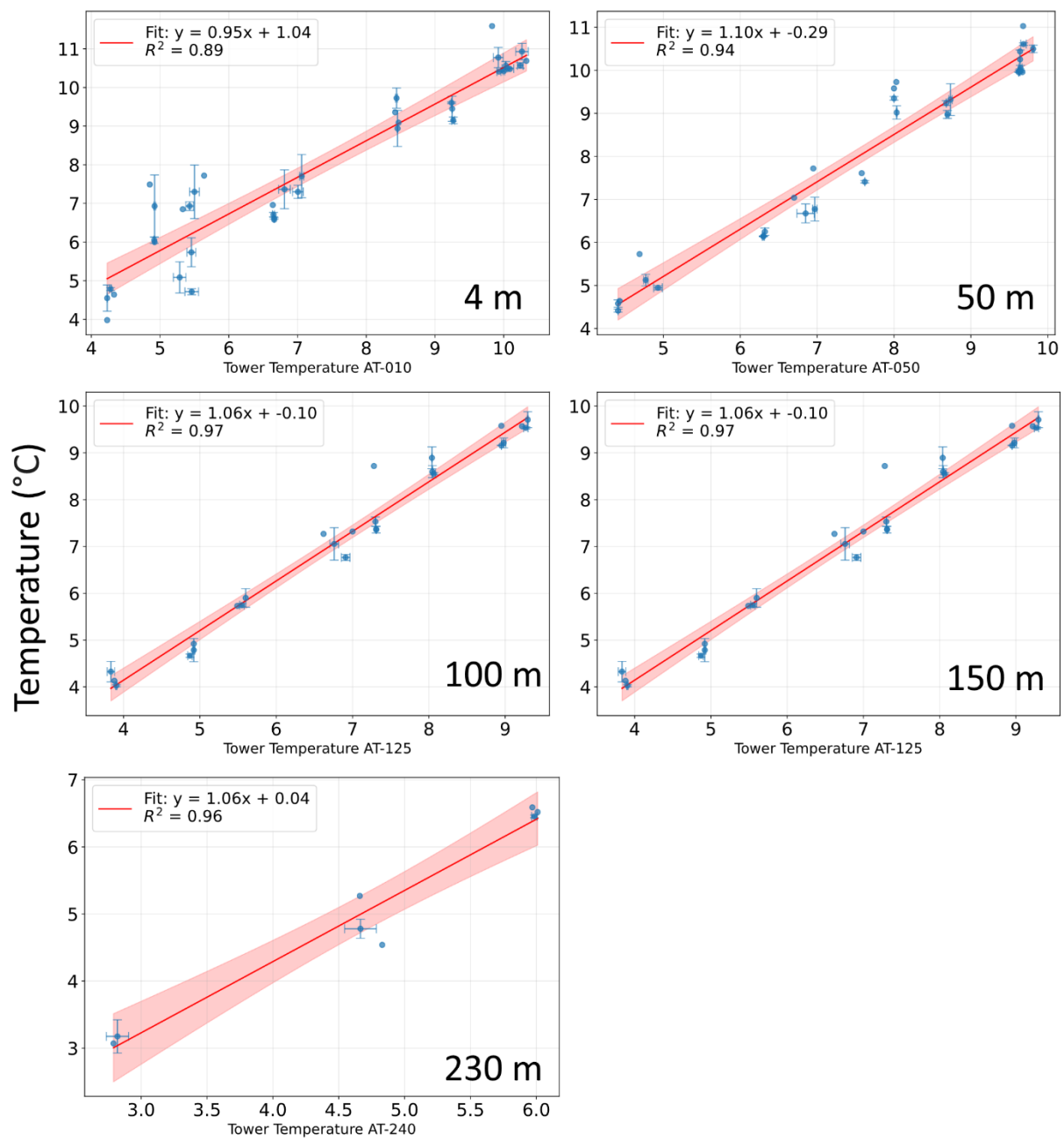
Figure S6. Correlation plot between temperature measurements obtained from the sensor placed on the drone with AE51 and from the sensors on the tower.
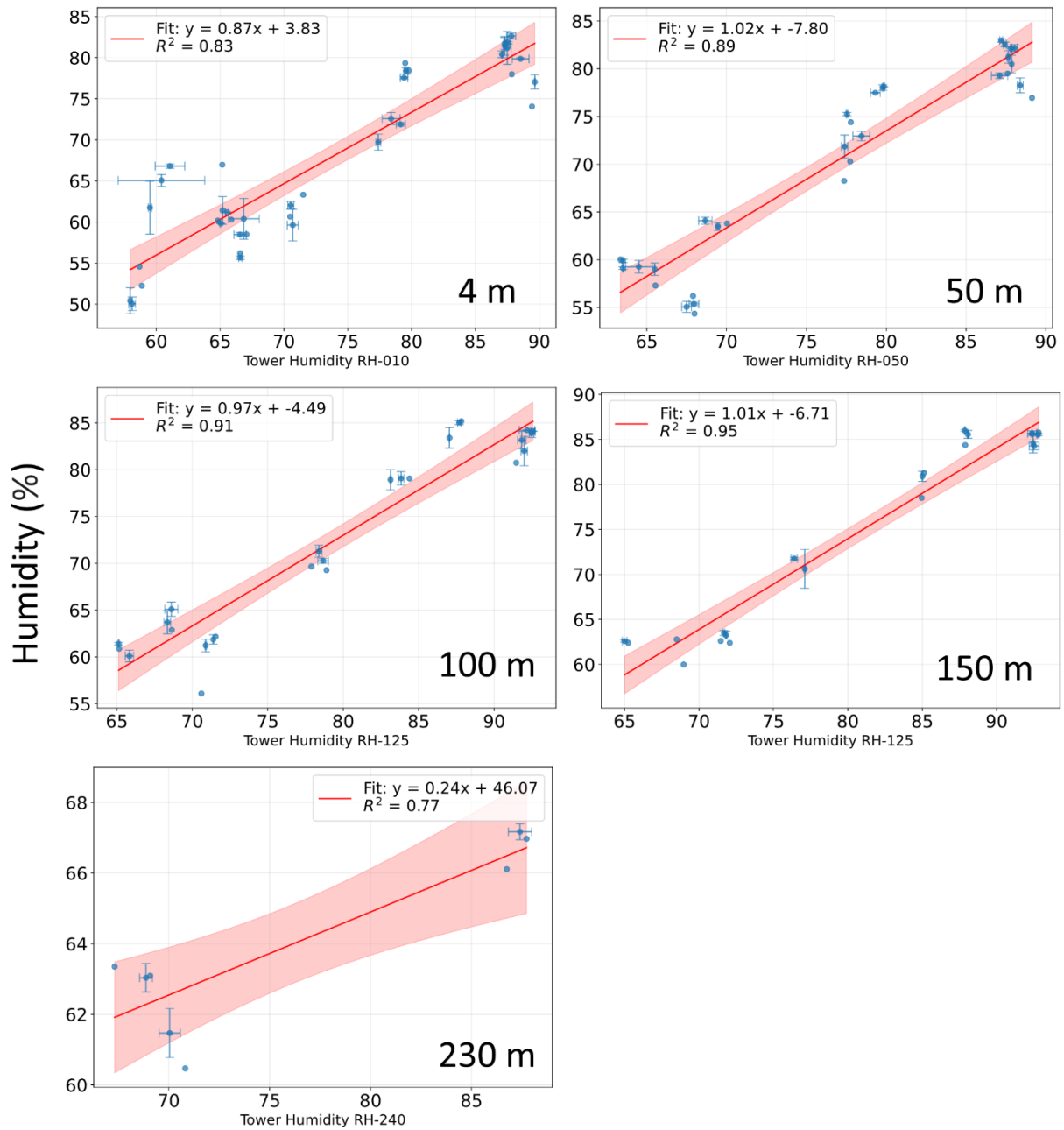
Figure S7. Correlation plot between relative humidity measurements obtained from the sensor placed on the drone with AE51 and from the sensors on the tower.

Table S1: Changes in concentrations for different devices and inlets (OPC, OPS, AE51) at various wind speeds and particle sizes (PM$_1$, PM$_{2.5}$, and PM$_{10}$). ↑ represents overestimation and ↓ represents underestimation

Device/Inlet type/Sampling	Loss	Inlet Diameter/ Flow Rate	Particle size range	WS (m/s)	PM1	PM2.5	PM10
OPC/Horizontal Inlet/Horizontal Sampling	Sampling Loss (%)	6 mm/ 0.28 L/min	0.35 – 10 μm	0 m/s	0 %	0 %	0 %
				2 m/s	10 % ↑	20 % ↑	110 % ↑
				4 m/s	20 % ↑	60 % ↑	390 % ↑
				6 m/s	40 % ↑	125 % ↑	750 % ↑
OPS/Vertical Inlet/Downward Sampling	Sampling Loss (%)	6.35 mm/ 1 L/min	0.3 – 10 μm	0 m/s	0 %	0 %	14 % ↓
				2 m/s	0 %	0 %	94 % ↓
				4 m/s	4 % ↑	6 % ↑	100 % ↓
				6 m/s	10 % ↑	12 % ↑	100 % ↓
AE51/Vertical Inlet/Downward Sampling	Whole Inlet (Particle Loss (%))	6.35 mm/ 1 L/min	0.01 – 2.5 μm	0 m/s	0 %	2 % ↓	NA
				2 m/s	2.5 % ↑	0 %	NA
				4 m/s	10 % ↑	4 % ↑	NA
				6 m/s	22.5 % ↑	3 % ↑	NA
AE51 Dryer/Vertical Inlet/Downward Sampling	Whole Inlet (Particle Loss (%))	6.35 mm/ 1 L/min	0.01 – 2.5 μm	0 m/s	0 %	0.6 %	NA
				2 m/s	5 % ↑	9 % ↑	NA
				4 m/s	18 % ↑	30 % ↑	NA
				6 m/s	35 % ↑	50 % ↑	NA
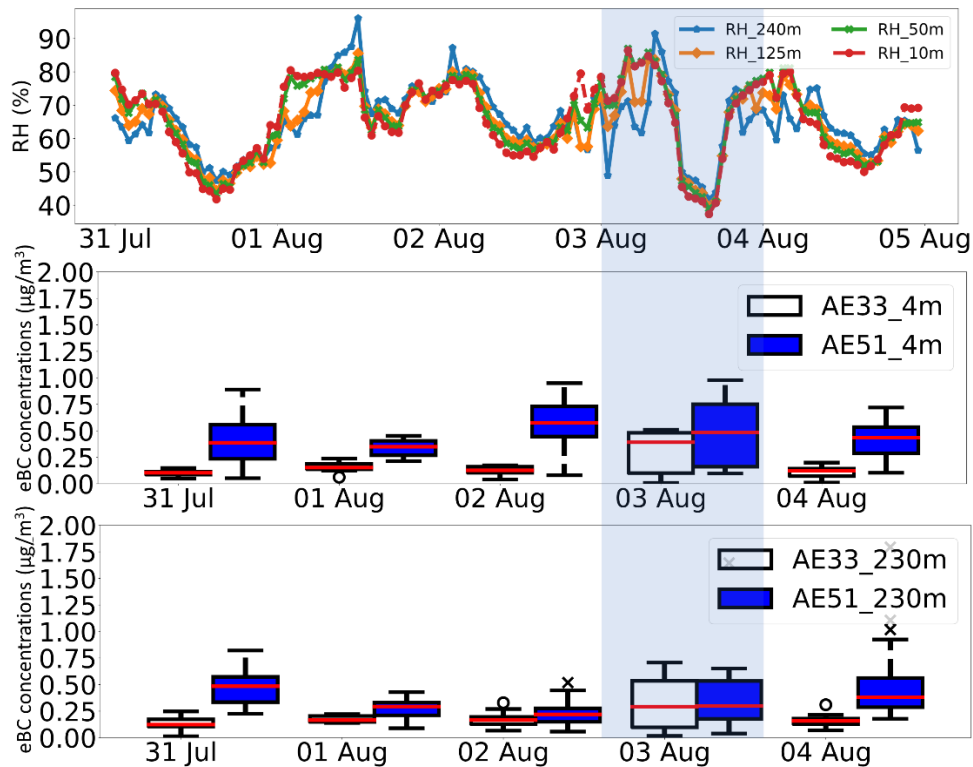
Figure S8. Variation of RH (top) from different heights of tower, eBC concentration from AE51 on drone and AE33 at 4m (middle) and 230m (bottom) during summer measurements at NAOK from July 31 to August 4, 2023.
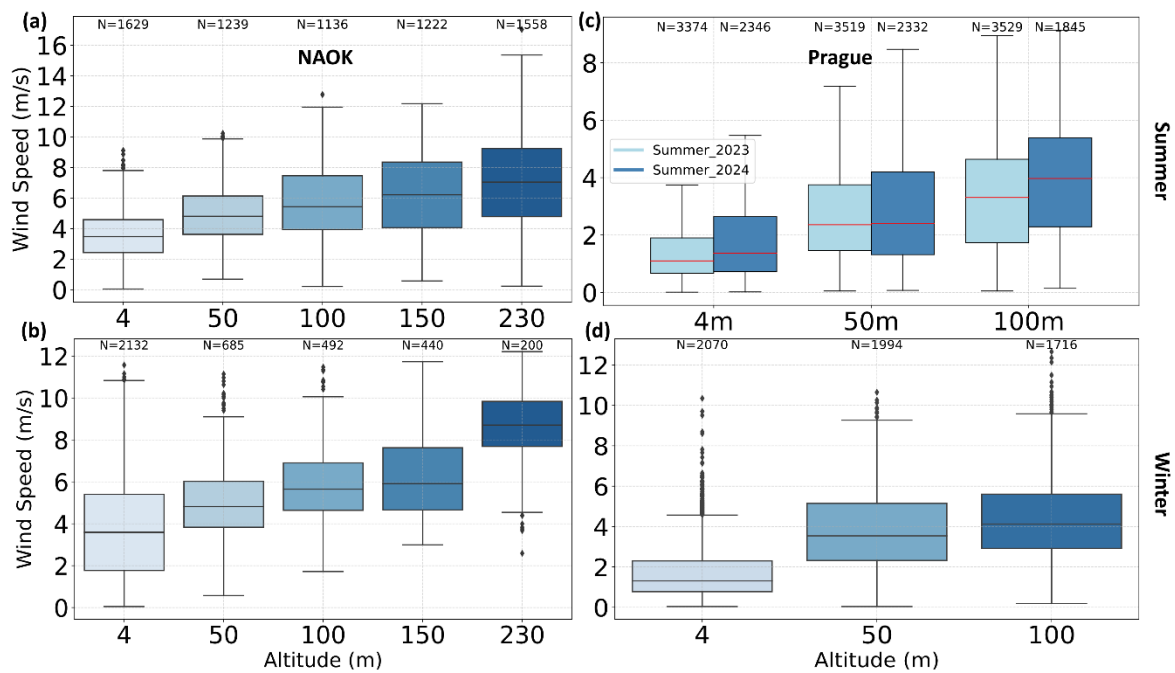
Figure S9. Wind speed at different altitudes from drone at NAOK during (a) summer 2023, (b) winter 2023 and at Prague in (c) summer 2023 and 2024, and (d) winter 2023.
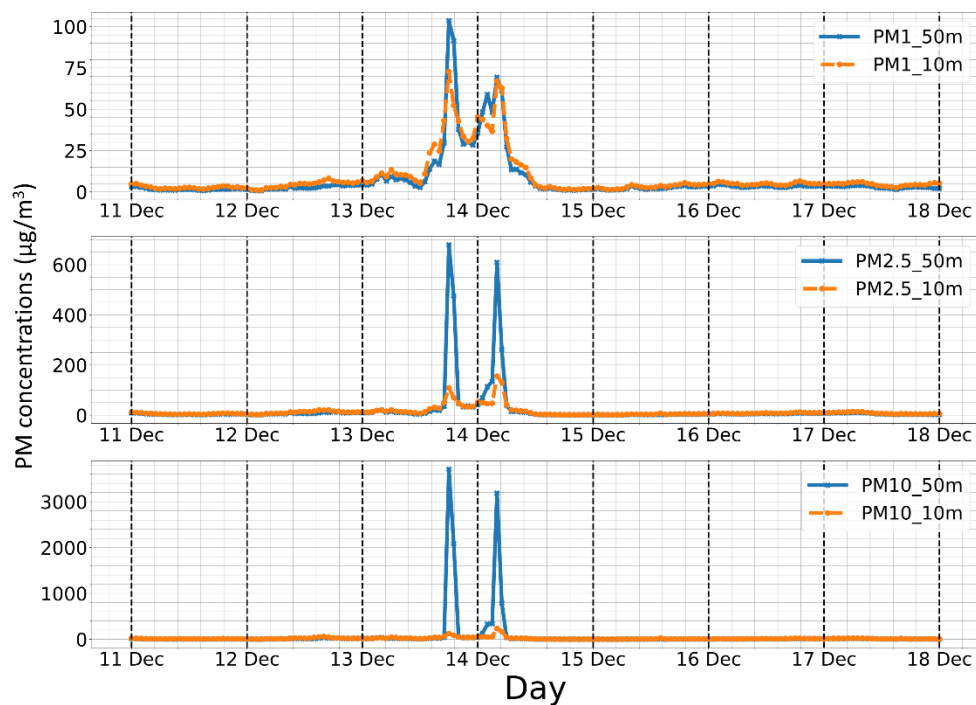
Figure S10. Variation of PM_1 (top), $PM_{2.5}$ (middle), and PM_{10} (bottom) at 10m (orange) and 50m (blue) at Prague during winter measurements from December 11 to December 17, 2023.

68
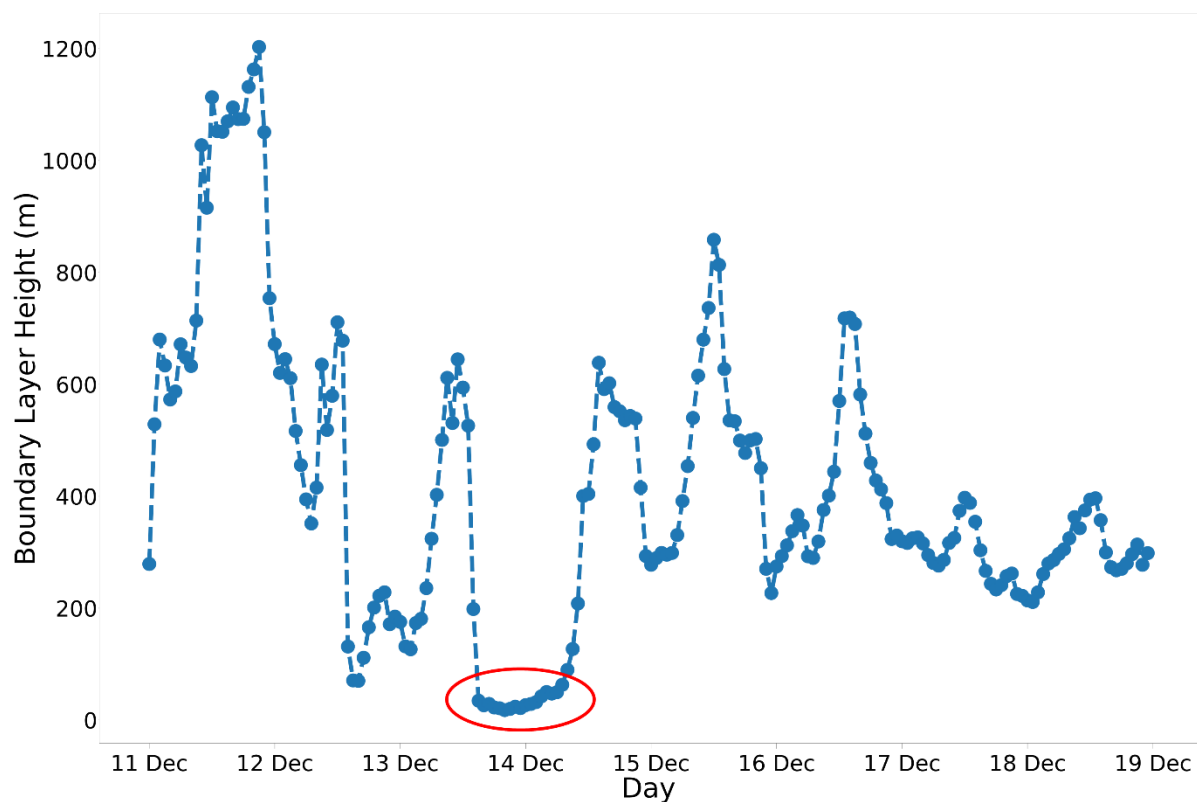
Figure S11. Variation of boundary layer height during winter campaign at Prague. The red circled area indicates the high pollution event.

69
70

71

72
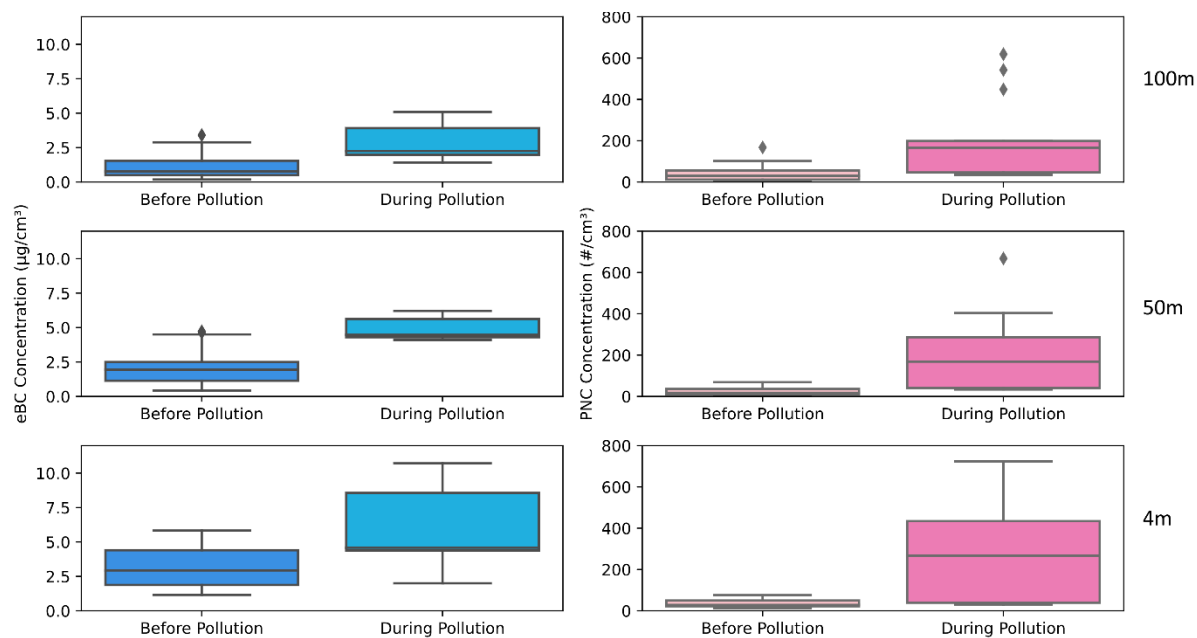
Figure S12. Boxplots of eBC mass concentration from AE51 and PNC from OPC on the drone before and during the high pollution event in Prague at 4 m, 50 m, and 100 m.

73
74

75
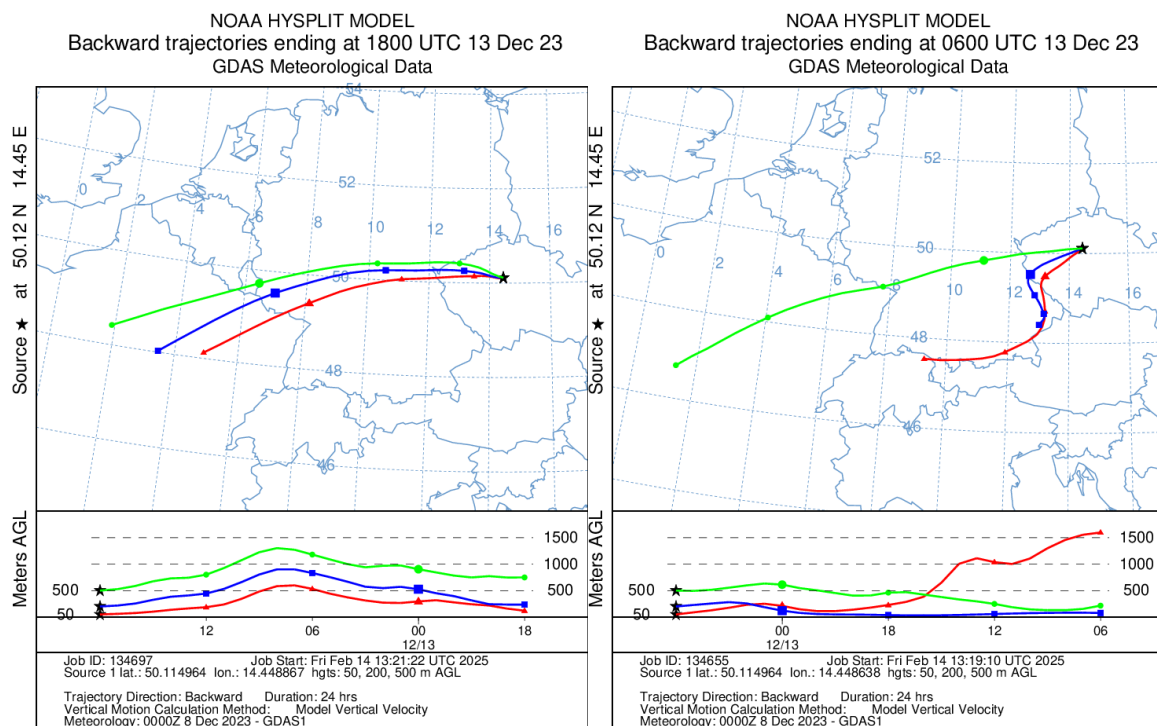
Figure S13. HYSPLIT back trajectories at various heights during high pollution episode (left) and before the episode (right).

79
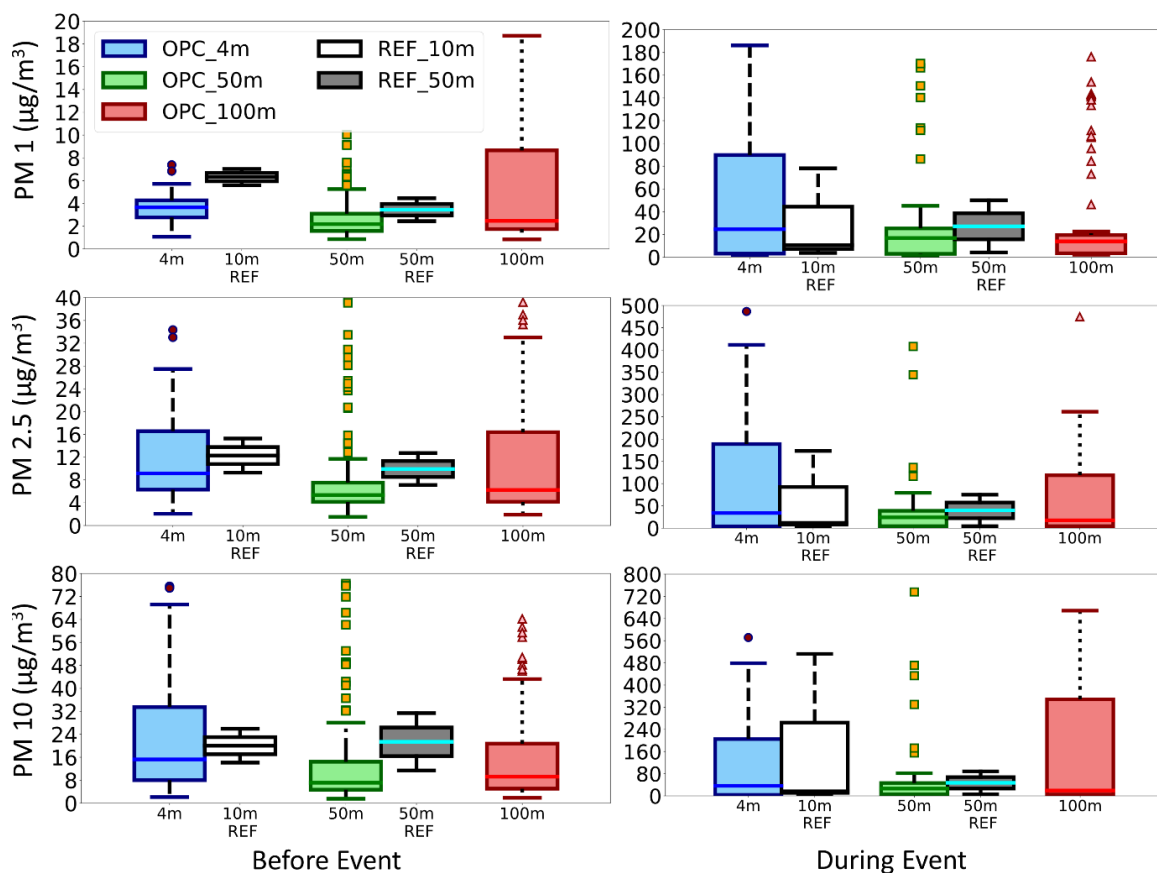
Figure S14. Boxplots comparing PM$_1$, PM$_{2.5}$, and PM$_{10}$ concentrations measured by the OPC on the drone and reference devices at 4 m, 50 m, and 100 m above ground level in Prague. Note different y-axis between left and right part of the plot.

83

84
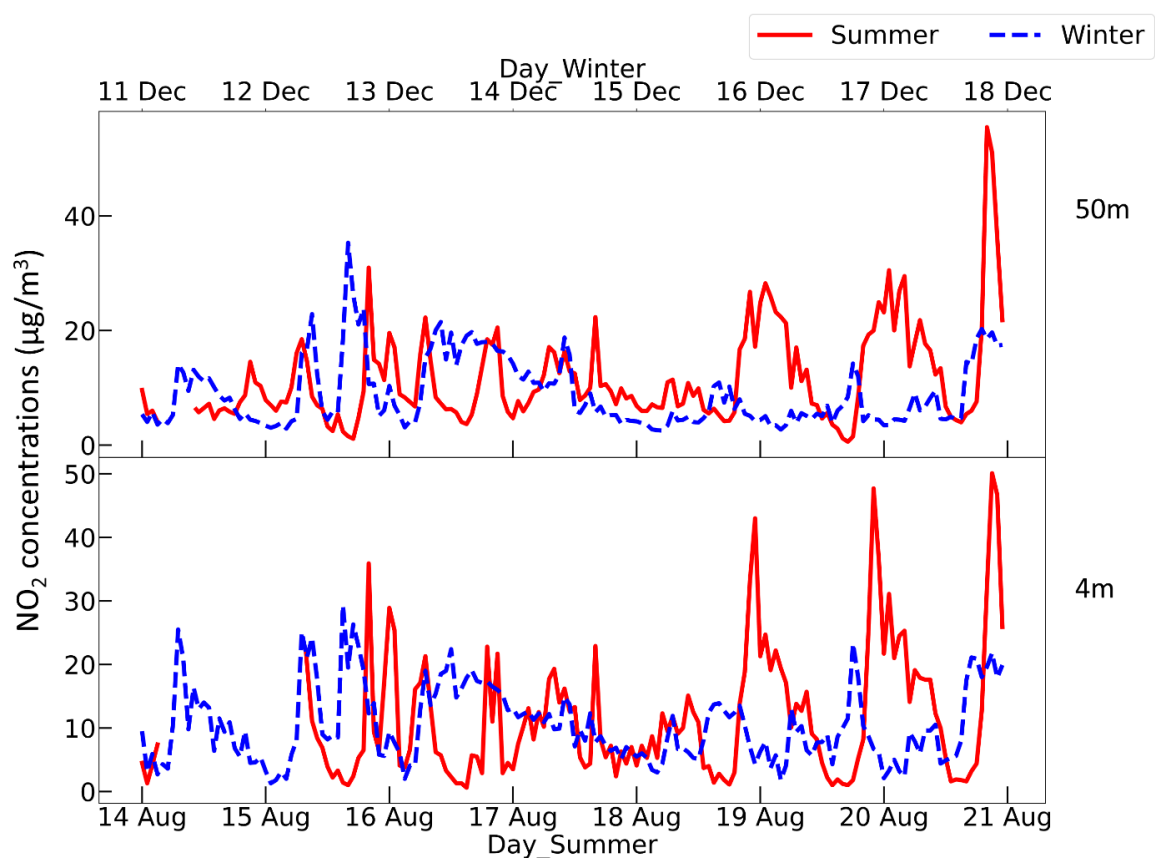
Figure S15. Variation of NO₂ concentrations during summer (red) and winter (blue) campaigns at 4m and 50m at Prague.

87
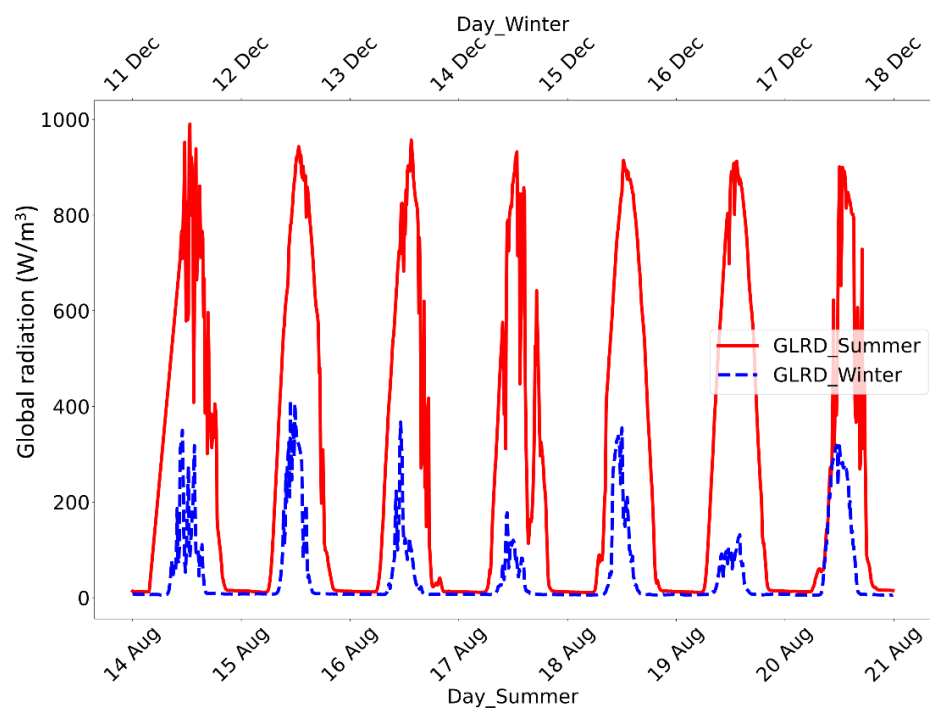
Figure S16. Variation of global radiation during summer (red) and winter (blue) campaign at Prague.